Transcorneal electrical stimulation promotes survival of retinal ganglion cells after optic nerve transection in rats...

Article *in* Brain research · August 2016

DOI: 10.1016/j.brainres.2016.08.034

CITATIONS
0

READS
32

12 authors, including:

Houfa Yin
Zhejiang University
19 PUBLICATIONS **33** CITATIONS
SEE PROFILE

Wei Zhang
Zhejiang University
31 PUBLICATIONS **81** CITATIONS
SEE PROFILE

Brain Research 1650 (2016) 10–20

Contents lists available at ScienceDirect

Brain Research

journal homepage: www.elsevier.com/locate/brainres

Research report

Transcorneal electrical stimulation promotes survival of retinal ganglion cells after optic nerve transection in rats accompanied by reduced microglial activation and TNF-α expression

Houmin Yin [a,1], Houfa Yin [b,c,1], Wei Zhang [d], Qi Miao [b,c], Zhenwei Qin [b,c], Shenchao Guo [b,c], Qiuli Fu [b,c], Jian Ma [b,c], Fang Wu [b,c], Jinfu Yin [b,c], Yabo Yang [b,c], Xiaoyun Fang [b,c,*]

[a] Department of Neurology, Second Affiliated Hospital of Zhejiang University School of Medicine, Hangzhou, Zhejiang Province, China
[b] Eye Center, Second Affiliated Hospital of Zhejiang University School of Medicine, Hangzhou, Zhejiang Province, China
[c] Zhejiang Provincial Key Laboratory of Ophthalmology, Hangzhou, Zhejiang Province, China
[d] Department of Orthopedics, Second Affiliated Hospital of Zhejiang University School of Medicine, Hangzhou, Zhejiang Province, China

ARTICLE INFO

Article history:
Received 16 April 2016
Received in revised form
20 August 2016
Accepted 24 August 2016
Available online 25 August 2016

Keywords:
Transcorneal electrical stimulation
Microglial activation
TNF-α
Optic nerve
Retinal ganglion cells

ABSTRACT

Microglial activation plays a crucial role in the pathological processes of various retinal and optic nerve diseases. TNF-α is a pro-inflammatory cytokine that is rapidly upregulated and promotes retinal ganglion cells (RGCs) death after optic nerve injury. However, the cellular source of TNF-α after optic nerve injury remains unclear. Thus, we aimed to determine the changes of retinal microglial activation in a rat model of optic nerve transection (ONT) after transcorneal electrical stimulation (TES). Furthermore, we assessed TNF-α expression after ONT and evaluated the effects of TES on TNF-α production. Rats were divided into 2 control groups receiving a sham surgery procedure, 2 ONT+Sham TES groups, and 2 ONT+TES groups. The rats were sacrificed on day 7 or 14 after ONT. RGCs were retrogradely labelled by Fluorogold (FG) 7 days before ONT, one TES group and corresponding controls were stimulated on day 0, 4, and the second were stimulated on day 0, 4, 7, 10. Whole-mount immunohistofluorescence, quantification of RGCs and microglia, and western blot analysis were performed on day 7 and 14 after ONT. TES significantly increased RGCs survival on day 7 and 14 after ONT, which was accompanied by reduced microglia on day 7, but not 14. TNF-α was co-localized with ameboid microglia and significantly increased on day 7 and 14 after ONT. TES significantly reduced TNF-α production on day 7 and 14 after ONT. Our study demonstrated that TES promotes RGCs survival after ONT accompanied by reduced microglial activation and microglia-derived TNF-α production.

1. Introduction

Microglia are highly specialized tissue macrophages of the central nervous system (CNS) and retina (Karlstetter et al., 2015). In the normal retina, microglia display a ramified morphology with many processes and play a critical role in immune surveillance and neuronal homeostasis (Karlstetter et al., 2010; Karlstetter et al., 2015). However, microglial activation represents a common pathomechanism underlying a variety of retinal and optic nerve diseases, including glaucoma, traumatic and hereditary optic neuropathies, and diabetic retinopathy (Gupta et al., 2003; Kyung et al., 2015; Liu et al., 2012; Zeng et al., 2008). Excessive or sustained microglial activation may result in irreversible neuronal loss due to chronic neuroinflammation (Karlstetter et al., 2010). Optic neuropathies induced by various types of stress and injury can lead to the progressive degeneration of retinal ganglion cells (RGCs) (Miki et al., 2013). Experimentally, optic nerve transection (ONT) is a commonly used in vivo model of RGCs degenerations in the adult CNS (Isenmann et al., 2003).

Tumor necrosis factor-alpha (TNF-α), a pro-inflammatory cytokine that is rapidly upregulated after optic nerve injury, ultimately leads to the death of RGCs (Ahmad et al., 2014; Cueva Vargas et al., 2015; Kyung et al., 2015; Tonari et al., 2012; Zheng et al., 2012). Similarly, intravitreal injections of TNF-α into normal eyes can also lead to RGCs death and optic nerve degeneration (Kitaoka et al., 2009). In the CNS, TNF-α can be released by

Abbreviations: BDNF, brain-derived neurotrophic factor; CNTF, ciliary nerve trophic factor; FG, Fluorogold; FGF-2, fibroblast growth factor beta; GCL, ganglion cell layer; GFAP, glial fibrillary acidic protein; GS, glutamine synthetase; Iba1, ionized calcium-binding adaptor molecule 1; IGF-1, insulin-like growth factor-1; IL-1β, interleukin-1beta; ONC, optic nerve crush; ONT, optic nerve transection; RGCs, retinal ganglion cells; RP, retinitis pigmentosa; TES, transcorneal electrical stimulation; TNF-α, tumor necrosis factor-alpha

* Corresponding author at: Eye Center, Second Affiliated Hospital of Zhejiang University School of Medicine, 88 Jiefang Road, Hangzhou 310009, China.
E-mail address: xiaoyunfang@zju.edu.cn (X. Fang).
[1] Houmin Yin and Houfa Yin contributed equally to this work.

http://dx.doi.org/10.1016/j.brainres.2016.08.034
0006-8993/

invading immune cells, activated astrocytes, or microglia and plays a central role in the pathogenesis of various degenerative diseases (de Kozak et al., 1997; Lebrun-Julien et al., 2009; Lieberman et al., 1989; Renz et al., 1988). However, the cellular source of TNF-α after ONT remains to be determined.

An increasing amount of evidence suggests that the inhibition of microglial activation could reduce the secretion of toxic cytokines and, thus, increase the survival of RGCs after optic nerve injury (Baptiste et al., 2005; Kyung et al., 2015; Roh et al., 2012; Yang et al., 2015). Electrical stimulation through different approaches has been shown to have neuroprotective effects on RGCs and photoreceptors (Morimoto et al., 2010; Pardue et al., 2005; Schatz et al., 2012; Zhou et al., 2012). Furthermore, Zhou et al. (2012) demonstrated that electrical stimulation ameliorates light-induced photoreceptor degeneration by suppressing the pro-inflammatory effects of microglia. However, to the best of our knowledge, no studies have investigated the effects of transcorneal electrical stimulation (TES) on retinal microglial response or its effects on the levels of TNF-α, a pro-inflammatory cytokine, after ONT. Thus, the present study investigated the changes of retinal microglial activation in a rat model of ONT after TES. Furthermore, this study also assessed the expression of TNF-α after ONT and examined the effects of TES on its production.

2. Results

2.1. TES promoted the survival of RGCs after ONT

First, we examined the effects of TES on RGCs survival after ONT. In the control group, the mean density of RGCs on day 7 after sham surgery procedure (2172 ± 110 cells/mm^2, n=5; Fig. 1A) did not significantly differ from that on day 14 after sham surgery procedure (2138 ± 96 cells/mm^2, n=5; Fig. 2A). However, the

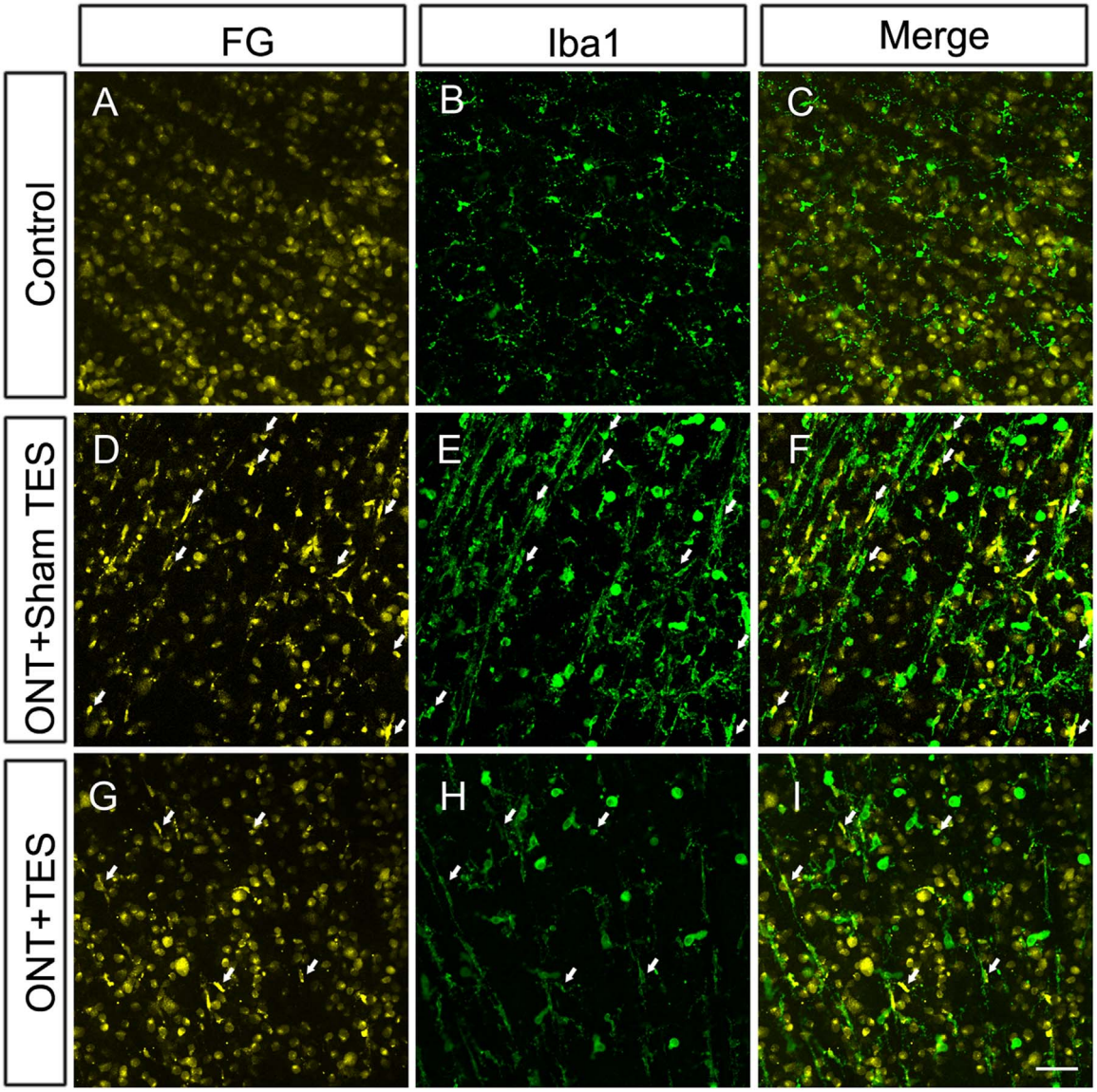

Fig. 1. Effects of TES on RGCs survival and microglial activation on day 7 after ONT. Double-labelled immunohistofluorescence for FG (RGCs) and Iba1 (microglia) in retinal whole-mounts at the GCL level in the central retina. (A-C) In the control group, FG-labelled RGCs exhibited typical circular or oval cell bodies, whereas Iba1-positive microglia maintained a ramified morphology. (D-F) In the ONT+Sham TES group, the number of FG-labelled RGCs was markedly lower than the number of RGCs in the control group, and FG-labelled phagocytic microglia (arrows) were rod-shaped or ameboid cells. Additionally, there was a significant increase in the number of Iba1-positive microglia, and these cells underwent a morphological change from a ramified form to either a rod or an ameboid form. Double-labelling of FG and Iba1 was observed in the rod or ameboid microglia (arrows). (G-I) TES significantly increased the number of FG-labelled RGCs and reduced the number of both FG-labelled phagocytic microglia (arrows) and Iba1-positive microglia. Scale bars: 50 μm.

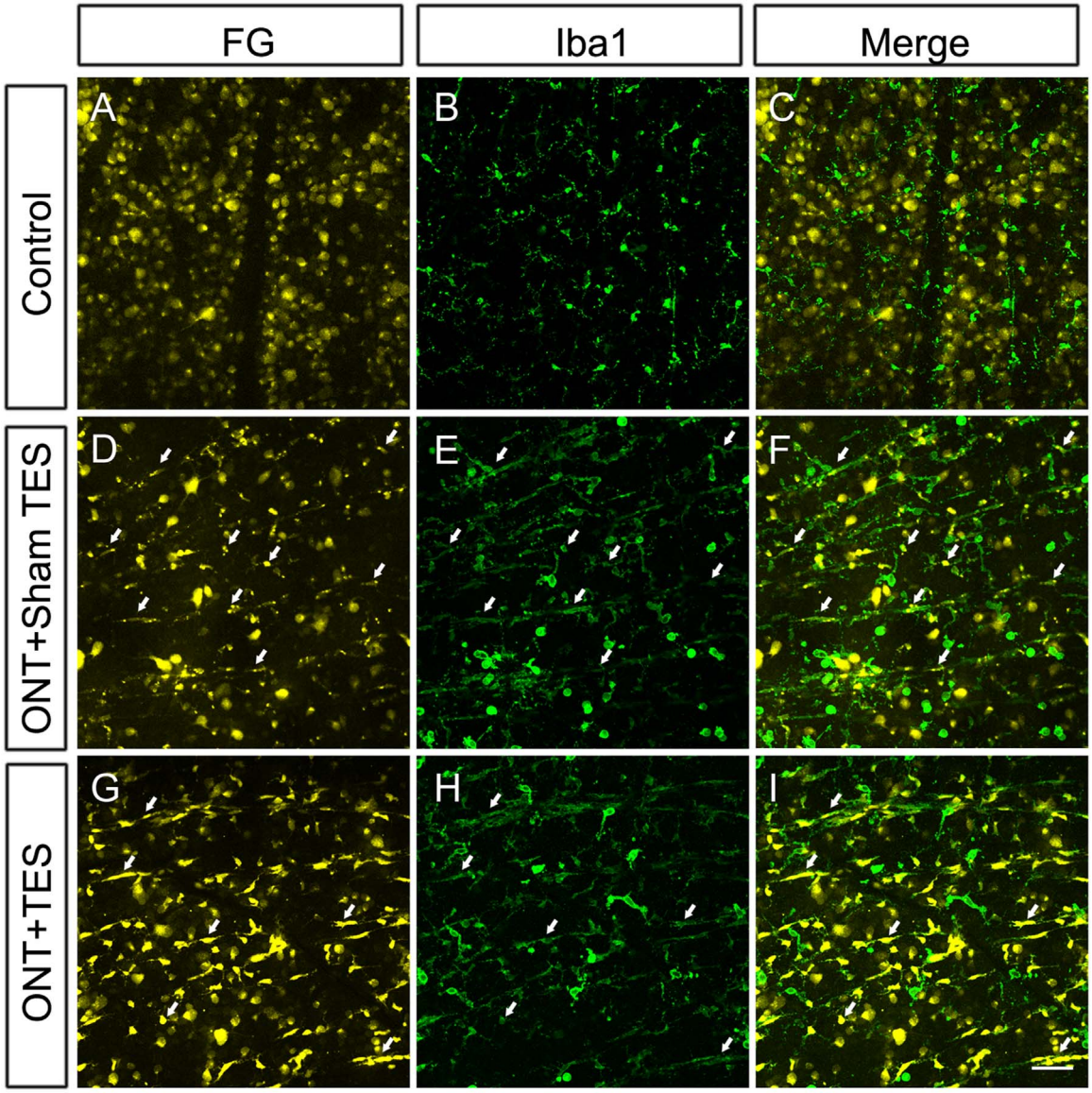

Fig. 2. Effects of TES on RGCs survival and microglial activation on day 14 after ONT. Double-labelled immunohistofluorescence for FG (RGCs) and Iba1 (microglia) in retinal whole-mounts at the GCL level in the central retina. (A-C) In the control group, FG-labelled RGCs exhibited typical circular or oval cell bodies, whereas Iba1-positive microglia maintained a ramified morphology. (D-F) In the ONT+Sham TES group, only a few FG-labelled RGCs were present, and double-labelling of FG and Iba1 was observed in the rod or ameboid microglia (arrows). (G-I) Although TES significantly increased the number of FG-labelled RGCs, the number of FG-labelled phagocytic microglia (arrows) or Iba1-positive microglia did not significantly differ from those in the ONT+Sham TES group. Scale bars: 50 μm.

mean density of RGCs in both control groups was significantly higher ($p < 0.001$, Fig. 7A) than that in the ONT+Sham TES group on day 7 (1140 ± 84 cells/mm^2, 52.5% of the control group, n=5; Fig. 1D) and day 14 (288 ± 37 cells/mm^2, 13.5% of the control group, n=5; Fig. 2D), and than the ONT+TES group on day 7 (1718 ± 101 cells/mm^2, 79.1% of the control group, n=5; Fig. 1G) and day 14 (781 ± 41 cells/mm^2, 36.5% of the control group, n=5; Fig. 2G) after ONT, respectively. However, retinas receiving TES had more surviving RGCs than the sham TES retinas on day 7 after ONT ($p < 0.001$, Fig. 7A). Similar to the results obtained on day 7 after ONT, the mean density of RGCs was significantly higher in the ONT+TES group than in the ONT+Sham TES group on day 14 after ONT ($p < 0.001$, Fig. 7A).

2.2. TES was accompanied by reduced microglial activation after ONT

FG-labelled phagocytic microglia were counted in the ganglion cell layer (GCL) on day 7 and 14 in each group. FG-labelled phagocytic microglia were not observed in the control groups on day 7 or 14 after sham surgery procedure (Figs. 1A and 2A). However, as expected, FG-labelled phagocytic microglia were apparent in the ONT+Sham TES group (Figs. 1D and 2D) and the ONT+TES group (Figs. 1G and 2G) on day 7 and 14 after ONT. On day 7 after ONT, the mean density of FG-labelled phagocytic microglia in the ONT+TES group (91 ± 6 cells/mm^2, n=5; Fig. 1G) was significantly lower than that in the ONT+Sham TES group (137 ± 18 cells/mm^2, n=5; $p=0.001$, Figs. 1D and 7B). However, on day 14 after ONT, the mean density of FG-labelled phagocytic microglia in the ONT+TES group (275 ± 21 cells/mm^2, n=5; Fig. 2G) did not significantly differ from that in the ONT+Sham TES group (287 ± 29 cells/mm^2, n=5; $p > 0.05$, Figs. 2D and 7B).

Because FG-labelled microglia represent only the microglia that have phagocytosed the fragments of dying RGCs labelled by FG, we used ionized calcium-binding adaptor molecule 1 (Iba1), a specific microglia marker, to further examine the changes of microglia in the GCL after ONT. In the control group, most Iba1-positive

microglia exhibited a ramified form with long processes extending from the cell bodies, whereas only a few Iba1-positive microglia with an ameboid morphology were identified (Figs. 1B and 2B). No double-labelling of FG and Iba1 was detected, which suggests that the microglia in the control group were in the "resting" state (Figs. 1C and 2C). Additionally, the number of microglia remained quite constant and did not significantly vary over time. The mean density of Iba1-positive microglia on day 7 after sham surgery procedure (128 ± 14 cells/mm^2, n=5) did not significantly differ from that on day 14 after sham surgery procedure (131 ± 11 cells/mm^2, n=5; $p > 0.05$). However, on day 7 and 14 after ONT, the number of Iba1-positive microglia increased and the morphology of the microglia changed from the ramified form to either the rod or the ameboid form in both the ONT+Sham TES group and the ONT+TES group (Figs. 1E, H and 2E, H).

Double-labelling of FG and Iba1 was observed in the rod or ameboid microglia (Figs. 1F, I and 2F, I). On day 7 after ONT, TES resulted in a significant reduction in the mean density of Iba1-positive microglia (228 ± 14 cells/mm^2, n=5; Fig. 1H) compared with the ONT+Sham TES group (282 ± 17 cells/mm^2, n=5; $p < 0.001$, Figs. 1E and 7C). However, on day 14 after ONT, there was no significant difference between the mean density of Iba1-positive microglia in the ONT+TES group (367 ± 32 cells/mm^2, n =5; Fig. 2H) and that in the ONT+Sham TES group (373 ± 19 cells/mm^2, n=5; $p > 0.05$, Figs. 2E and 7C). However, the number of Iba1-positive microglia was significantly increased in both the ONT+Sham TES group and the ONT+TES group compared to the control group on day 7 and 14 after ONT ($p < 0.001$, respectively, Fig. 7C).

2.3. Identification of TNF-α-generating cells in the GCL after ONT

To identify TNF-α-generating cells in the GCL, TNF-α was localized in retinal whole-mounts with the cell markers Iba1 (microglia), glial fibrillary acidic protein (GFAP; astrocytes), and glutamine synthetase (GS; Müller cells). In the control group, astrocytes and Müller cells were in a resting state, ramified microglia were distributed in a mosaic pattern, with very few ameboid microglia on day 7 after sham surgery procedure (Figs. 3A1, A2; 4A1, A2 and 5A1, A2). Moreover, very few TNF-α positive cells were detected (Figs. 3B1, B2; 4B1, B2 and 5B1, B2). However, in the ONT+Sham TES group, astrocytes and Müller cells were activated as indicated by the increased intensities of GFAP immunoreactivity and GS immunoreactivity on day 7 after ONT (Figs. 4D1, D2 and 5D1, D2). Furthermore, microglia were activated and changed their morphology from ramified to either the rod or ameboid form (Fig. 3D1, D2). Of note, TNF-α was co-localized with ameboid microglia, but not with rod microglia, astrocytes or Müller cells (Figs. 3F1, F2; 4F1, F2 and 5F1, F2), which indicates that ameboid microglia are the source of TNF-α after ONT. On day 14 after ONT, TNF-α was still co-localized with ameboid microglia (Fig. 6F1, F2).

2.4. TES was accompanied by reduced expression of TNF-α in microglia after ONT

As shown in Figs. 3–6, TNF-α labelling identified the location of TNF-α production, which indicates that TNF-α is primarily expressed in ameboid microglia after ONT. Furthermore, western blot analysis revealed significantly increased expression of TNF-α in the ONT+Sham TES group compared to the control group on day 7 and day 14 after ONT (n=5; $p < 0.001$, Fig. 8). However, TES significantly decreased the expression of TNF-α in the ONT+TES group on day 7 and day 14 after ONT (n=5; $p < 0.001$ and $p < 0.01$, respectively, Fig. 8).

3. Discussion

Previous studies have demonstrated that microglial activation and the release of pro-inflammatory cytokines are involved in

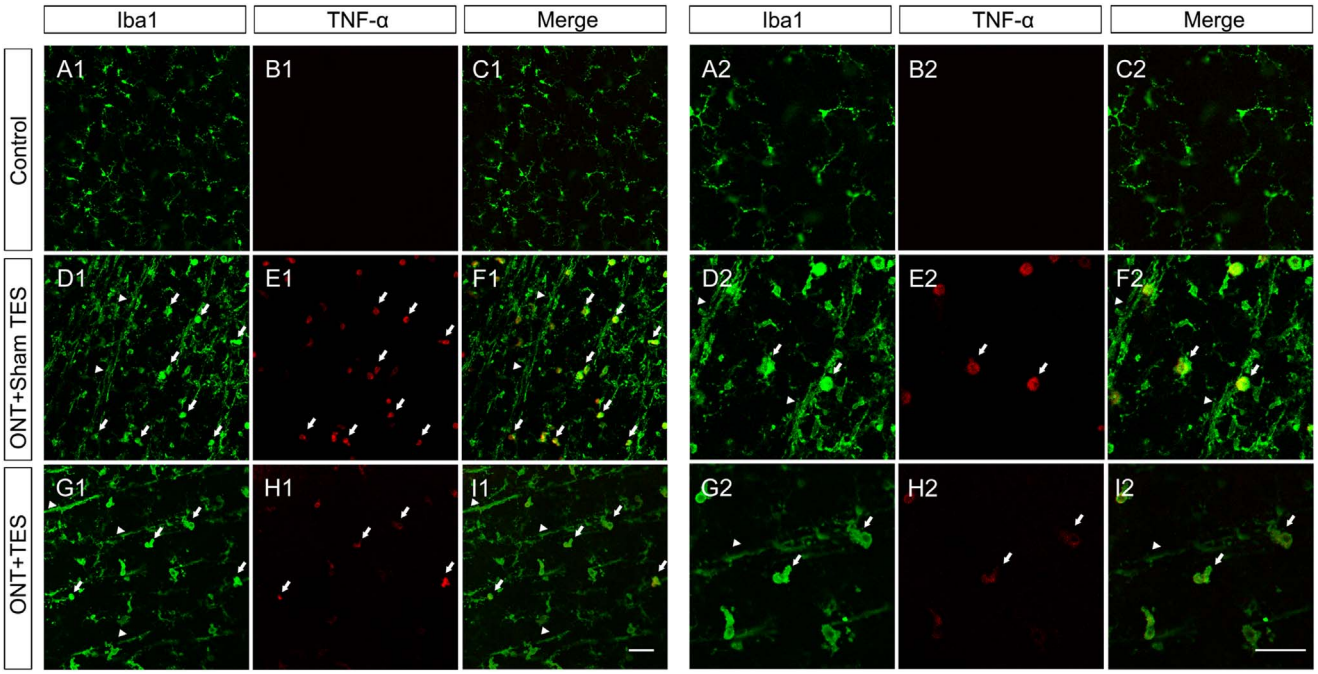

Fig. 3. Identification of TNF-α-generating cells in the GCL and assessment of the effects of TES on microglial activation on day 7 after ONT. Double-labelled immunohistofluorescence for Iba1 (microglia) and TNF-α in retinal whole-mounts at the GCL level in the central retina. (A1-C1) In the control group, Iba1-positive microglia maintained a ramified morphology, and only a few TNF-α-positive cells were observed. (D1-F1) On day 7 after ONT, there was a significant increase in the number of microglia, and these cells underwent a morphological change from a ramified form to either a rod (arrowheads) or an ameboid (arrows) form. Double-labelling of Iba1 and TNF-α was observed in only ameboid microglia (arrows). (G1-I1) On day 7 after ONT, TES was accompanied by reduced microglial activation and the number of TNF-α-generating cells (arrows). (A2-C2, D2-F2, G2-I2) Higher-magnification versions of the left panels. Scale bars: 50 μm.

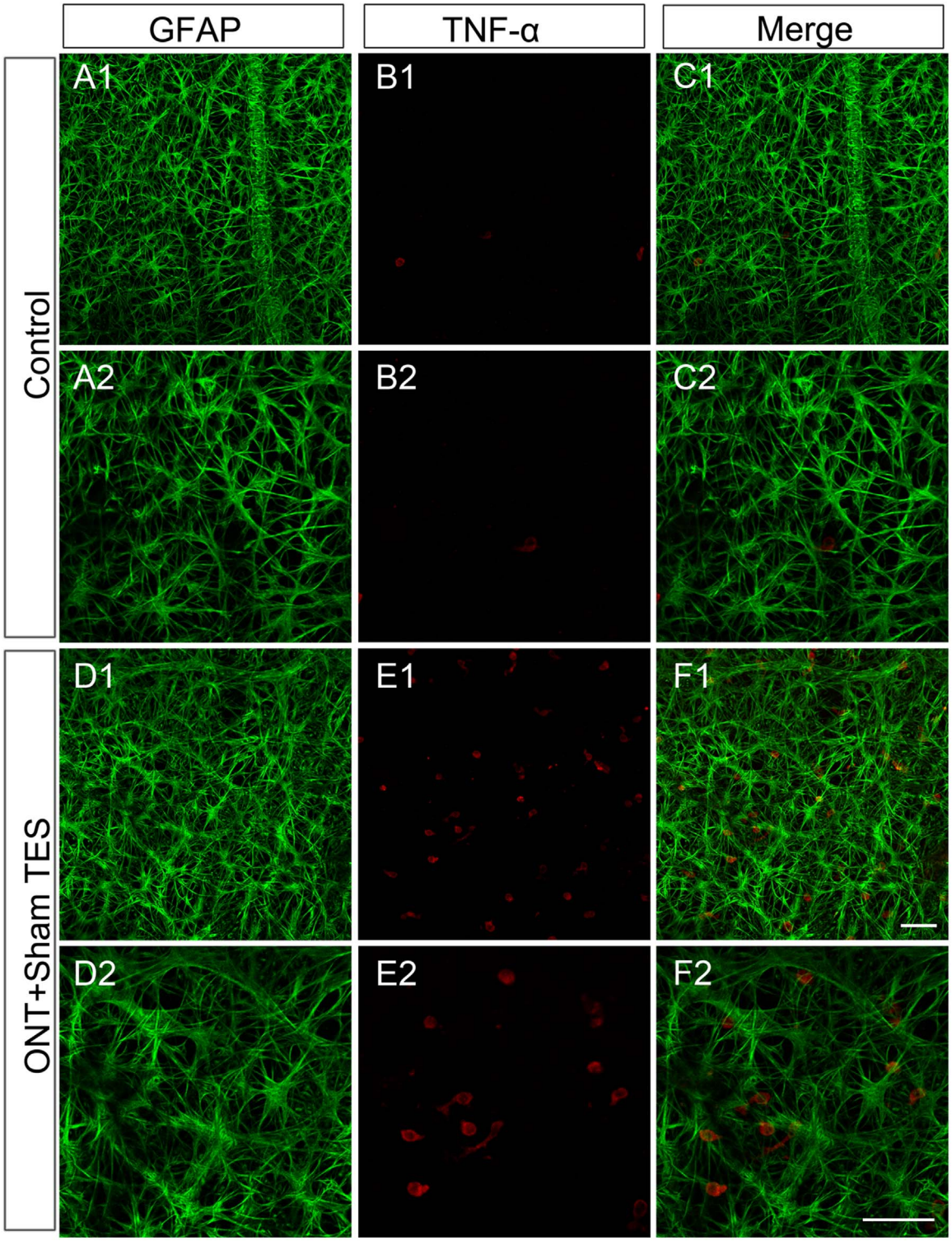

Fig. 4. Identification of TNF-α-generating cells in the GCL after ONT. Double-labelled immunohistofluorescence for GFAP (astrocytes) and TNF-α in retinal whole-mounts at the GCL level in the central retina on day 7 after ONT. (A1-C1) In the control group, only a few TNF-α-positive cells were observed. (D1-F1) The labelling intensity of GFAP increased after ONT, but TNF-α was not co-localized with GFAP. (A2-C2, D2-F2) Higher-magnification versions of the upper panels. Scale bars: 50 μm.

RGCs death after optic nerve injury (Ahmad et al., 2014; Tezel et al., 2004). Microglial activation has dual effects. In the early stages of injury, microglial activation can exert protective functions via the phagocytosis of cell debris and the release of protective molecules, such as insulin-like growth factor-1 (IGF-1). However, excessive or prolonged microglial activation can have harmful effects via the induction of chronic inflammation and the release of pro-inflammatory cytokines, such as TNF-α and interleukin-1 beta (IL-1β), which can result in irreversible neuronal death (Cuenca et al., 2014).

In the present study, ONT-induced damage led to a continuous and significant loss of RGCs and a significant increase of retinal microglia. However, TES promoted RGCs survival accompanied by reduced microglial activation. On day 7 and 14 after ONT, 52.5%

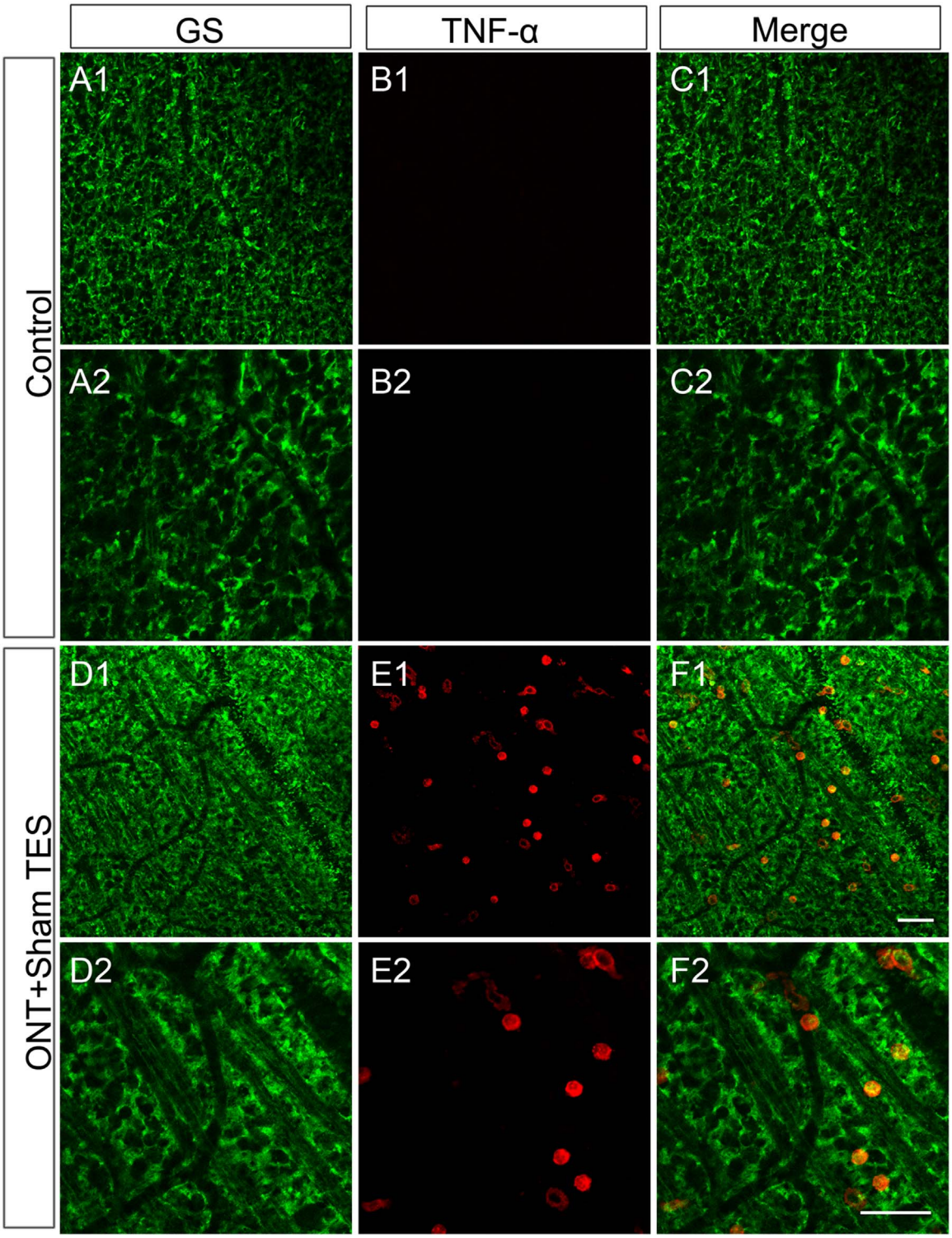

Fig. 5. Identification of TNF-α-generating cells in the GCL after ONT. Double labelled immunohistofluorescence for GS (Müller cells) and TNF-α in retinal whole-mounts at the GCL level in the central retina on day 7 after ONT. (A1-C1) In the control group, only a few TNF-α-positive cells were observed. (D1-F1) The labelling intensity of GS increased after ONT, but TNF-α was not co-localized with GS. (A2-C2, D2-F2) Higher-magnification versions of the upper panels. Scale bars: 50 μm.

and 13.5% of the original population of RGCs survived, respectively, which is similar to the findings of previous report (Morimoto et al., 2010). However, in the present study, TES increased the percentages of surviving RGCs to 79.1% and 36.5% on day 7 and 14, respectively, after ONT. These survival rates were lower than those reported by Morimoto et al. (2010) on day 7 and 14 after ONT (85.4% and 47.1%, respectively), but the TES parameters used in the present study were not identical to the optimal parameters used in that previous study. This may explain the observed differences in the RGC survival percentages.

Microglial activation occurs early after optic nerve injury (Cen et al., 2015; Liu et al., 2012; Slusar et al., 2013; Yuan et al., 2015), in this regard, the present results are in agreement with those of previous studies. After ONT, there were increases in the numbers of both FG-labelled microglia and Iba1-positive microglia, as well as changes from the ramified form of these cells to either the rod

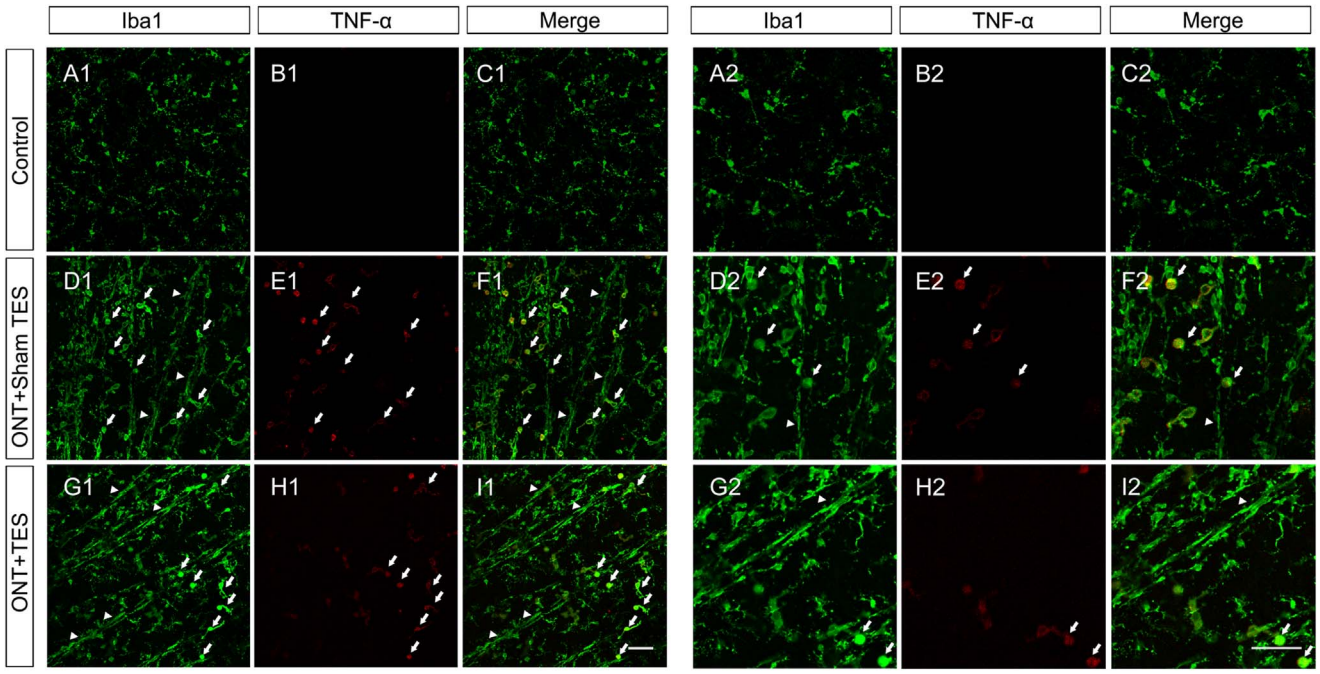

Fig. 6. Assessment of the effects of TES on microglial activation on day 14 after ONT. Double-labelled immunohistofluorescence for Iba1 (microglia) and TNF-α in retinal whole-mounts at the GCL level in the central retina. (A1-C1) In the control group, Iba1-positive microglia maintained a ramified morphology, and only a few TNF-α-positive cells were observed. (D1-F1) On day 14 after ONT, there was a significant increase in the number of microglia, and these cells underwent a morphological change from a ramified form to either a rod (arrowheads) or an ameboid (arrows) form. Double-labelling of Iba1 and TNF-α was observed in only ameboid microglia (arrows). (G1-I1) On day 14 after ONT, microglial activation was similar to that in the ONT + Sham TES group after TES. (A2-C2, D2-F2, G2-I2) Higher-magnification versions of the left panels. Scale bars: 50 μm.

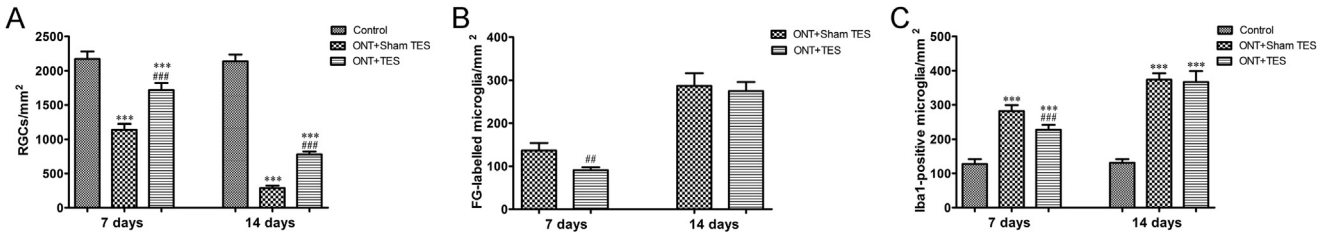

Fig. 7. Quantification of the numbers of RGCs and microglia in different groups on day 7 and 14 after ONT. (A) FG-labelled RGCs, (B) FG-labelled phagocytic microglia, and (C) Iba1-positive microglia. The bars represent the mean ± SD. $^{***}P < 0.001$ vs. the control group, $^{\#\#\#}P < 0.001$ vs. the ONT + Sham TES group, and $^{\#\#}P < 0.01$ vs. the ONT + Sham TES group.

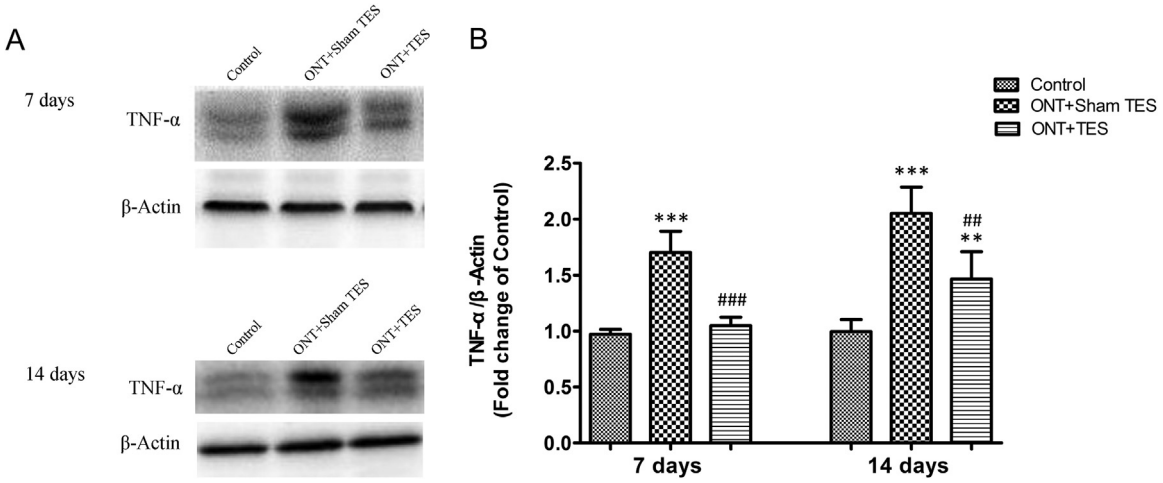

Fig. 8. Western blot analysis of TNF-α protein levels in different groups on day 7 and 14 after ONT. (A) Representative bands immunoreactive for TNF-α and β-actin. (B) Densitometry of the TNF-α-immunoreactive bands. Data were normalized to β-actin levels in the same sample and expressed as the fold change of the control value. The bars represent the mean ± SD. $^{***}P < 0.001$ vs. the control group, $^{**}P < 0.01$ vs. the control group, $^{\#\#\#}P < 0.001$ vs. the ONT + Sham TES group, and $^{\#\#}P < 0.01$ vs. the ONT + Sham TES group.

or the ameboid form. On day 7 after ONT, rod microglia were aligned with each other and scavenged the RGCs debris via phagocytosis. However, ameboid microglia were the major TNF-α-generating cells, which indicates that these cells might exert different effects. Yuan et al. (2015) has reported that rod microglia appear at approximately 7 days after ONT and peak during 14 to 21 days. Similarly, the present study showed that microglial activation was much more evident on day 14 after ONT and that this occurred in conjunction with the loss of most RGCs after ONT, as almost 90% RGCs would be lost at day 14.

It is well documented that electrical stimulation can enhance the survival of RGCs or photoreceptors as well as promote axonal regeneration in various animal models, such as retinitis pigmentosa (RP), optic nerve injury (crush or axotomy), light-induced retinal damage and ischemic retinal damage (Henrich-Noack et al., 2013; Miyake et al., 2007; Morimoto et al., 2007, 2010; Okazaki et al., 2008; Schatz et al., 2012; Wang et al., 2011). Moreover, several studies have demonstrated that TES benefits patients with RP or RGCs damage stemming from non-arteritic ischemic optic neuropathy, traumatic optic neuropathy and retinal artery occlusion (Fujikado et al., 2006; Inomata et al., 2007; Schatz et al., 2011). However, the relationship between the number of surviving RGCs and vision restoration is not one-to-one relationship (Henrich-Noack et al., 2013). TES-induced neuroprotection after severe optic nerve crush (ONC) was not associated with improved vision recovery (Henrich-Noack et al., 2013). It is likely that severe ONC may lead to irreversible degeneration of axons, precluding any functional recovery (Henrich-Noack et al., 2013). In contrast, after mild ONC, TES would induce a rapid functional recovery of visually evoked potentials and protect retinal axons from the ensuing degeneration (Miyake et al., 2007).

The neuroprotection of electrical stimulation is believed to involve the release of endogenous growth factors, such as IGF-1, brain-derived neurotrophic factor (BDNF), fibroblast growth factor beta (FGF-2), and ciliary nerve trophic factor (CNTF), as well as the enhancement of the intrinsic sensitivity of neurons to these factors (Ciavatta et al., 2009; Morimoto et al., 2005; Ni et al., 2009). Additionally, recent study evaluating electrical stimulation has reported its prominent inhibitory effects on the secretion of TNF-α and IL-1β in microglia, which has been shown to ameliorate light-induced photoreceptor degeneration in vitro (Zhou et al., 2012). Similarly, the present data showed that TES was accompanied by reduced microglial activation and TNF-α expression at 7 days after ONT. Although the difference of microglial activation at 14 days after ONT was not significant with or without TES treatment, there was still a reduction in the expression of TNF-α.

Although microglia have been implicated as the major source of TNF-α in neurodegenerative disorders, numerous studies have demonstrated that astrocytes, Müller cells, and neurons may also be a source of TNF-α (de Kozak et al., 1997; Lebrun-Julien et al., 2009; Lieberman et al., 1989; Renz et al., 1988). However, the present study was the first to demonstrate that Iba1-positive microglia are the major source of TNF-α after ONT and that TNF-α is primarily expressed in ameboid microglia rather than in rod microglia; nonetheless, astroglial activation and Müller cell activation were also observed. Taken together, these findings indicate that activated ameboid microglia should be considered an important factor in the pathophysiology of RGCs death. Therefore, it is reasonable to hypothesize that the accompanying reduction of microglial activation and TNF-α expression after TES may play important roles in neuroprotection following ONT. Of interest, Cueva Vargas et al. (2015) reported an upregulation of TNF-α in Müller cells and microglia/macrophages with ameboid shape in a rat model of ocular hypertension. In the present study, ameboid microglia were the primary TNF-α-generating cells and it can be speculated that the use of various models of injury resulted in the disparities among studies.

It is currently unknown how TES alter microglia behavior, but it might involve mechanisms dependent on transmembrane voltage-gated ion channel activity (Zhou et al., 2012). Previous studies have shown that changes in voltage-gated calcium (Ca^{2+}) channels and Ca^{2+} influx induced by electrical stimulation led to increased neurotrophic factors release from neurons and glia cells (Sato et al., 2008; Sharma et al., 2010; Wenjin et al., 2011). Moreover, microglial ion channels, such as rectifier potassium (K^{+}) channels and Ca^{2+}-activated K^{+} channels, are capable of modulating cytokine secretion from microglia (Eder, 2005, 2010). In addition, Ca^{2+} influx in microglia plays a pivotal role in microglial activation and their associated functions (Sharma and Ping, 2014). It is plausible, however, that the decrease of microglial activation after ONT observed in the present study may be related to the enhanced survival of RGCs by TES. In line with previous studies, TES in the present study may only delay RGCs degeneration, which contributed to the delayed rise in microglial activation and TNF-α expression (Henrich-Noack et al., 2013; Miyake et al., 2007; Okazaki et al., 2008). Therefore, additional studies using whole-cell patch clamp techniques and various channel blockers are necessary to determine the potential mechanisms.

In conclusion, the present study demonstrated that TES promotes RGCs survival after ONT accompanied by reduced microglial activation and the expression of microglia-derived TNF-α. As microglial activation and TNF-α release play prominent roles in optic neuropathies, TES might be a valuable therapeutic approach to the treatment of these disorders.

4. Experimental procedure

4.1. Animals

Adult male Sprague-Dawley rats (220–250 g) were obtained from Slac Laboratory Animal Co., Ltd. (Shanghai, China). The animals were maintained on a 12 h light-dark cycle under controlled temperature and humidity conditions with food and water ad libitum. All procedures were approved by the Animal Ethics Committee of the Second Affiliated Hospital of Zhejiang University School of Medicine and were in accordance with the National Institutes of Health Guide for the Care and Use of Animals and the ARVO Statement for the Use of Animals in Ophthalmic and Vision Research. The rats were anesthetized with an intraperitoneal injection of sodium pentobarbital (50 mg/kg) for all surgical procedures.

Rats were randomly divided into 6 groups: 2 control groups receiving a sham surgery procedure, 2 sham TES groups receiving sham TES treatment after ONT (ONT+Sham TES group), and 2 TES groups receiving TES treatment after ONT (ONT+TES group). The rats were sacrificed on day 7 or 14 after ONT.

4.2. Retrograde labelling of RGCs

RGCs were retrogradely labelled by FG (Fluorochrome LLC; Denver, CO, USA) 7 d prior to ONT, as previously described (Siddiqui et al., 2014). Briefly, the rats were anesthetized and placed in a stereotactic device. Labelling was performed by injecting 2 μL of 2% FG into the superior colliculus using a 10 μL Hamilton syringe.

4.3. ONT procedure

All surgeries were performed on the right eye only and the left eye was not manipulated. The reason was that unilateral injury to the optic nerve has been shown to induce a microglial response in the contralateral eye (Cen et al., 2015; Galindo-Romero et al., 2013;

Wang et al., 2015). ONT was performed as previously described (Slusar et al., 2013). Briefly, the rats were anesthetized as described above, and the superior surface of the right eye was exposed by an incision along the superior orbital margin. Then, the optic nerve was approached by partially resecting the lacrimal gland and the superior rectus muscle, and the optic nerve sheath was exposed longitudinally 1–2 mm posterior to the globe. The optic nerve was carefully transected approximately 1 mm behind the globe with Vannas scissors. Fundus examination was performed immediately after ONT and before sacrifice to check the integrity of the retinal blood supply. In the control group, a sham surgery procedure (exposing the optic nerve sheath but without transecting the optic nerve) was performed on the right eye. Rats showing signs of permanent ischemia were excluded from the study.

4.4. TES procedure

A ring-shaped gold electrode (Roland Consult; Brandenburg, Germany) was used as the TES stimulating electrode, and the reference electrode was placed in the subcutaneous tissue of the ipsilateral forehead using a needle. For stimulation, the rats were anaesthetized by 0.4% oxybuprocaine eye drops in addition to systemic anesthesia described above. The gold electrode was placed on the cornea with Vidisic optical gel (M. Pharma; Berlin, Germany) to protect the cornea and maintain good electrical contact. The electrical stimulation was performed with an Isolated Pulse Generator (A-M Systems; Sequim, WA, USA). We used a stimulation protocol modified from Morimoto et al. (2010). Using this protocol, 20 Hz biphasic rectangular current pulses of 2 ms/phase were delivered from the electrical stimulation system to the gold electrode. The current intensities were 0 (ONT+Sham TES group) and 200 μA (ONT+TES group) with a stimulation duration of 60 min. The treatment was applied either on day 0 and 4, or on day 0, 4, 7 and 10 after ONT. To be specific, there were two ONT+TES groups, one was stimulated on day 0 and 4 and sacrificed on day 7, and another was stimulated on day 0, 4, 7 and 10 and sacrificed on day 14, as well as two corresponding ONT+Sham TES groups. Meanwhile, there were two corresponding control groups, one was sacrificed on day 7, and another was sacrificed on day 14.

4.5. Tissue preparation

On day 7 and 14 after ONT, rats were euthanized by an overdose of sodium pentobarbital (240 mg/kg) via intraperitoneal injection and then transcardially perfused with phosphate buffered saline (PBS), followed by 4% paraformaldehyde (PFA). Their eyes were then immediately enucleated. For whole-mount immunohistofluorescence analysis, the retinas were dissected from the choroids, cut into four quadrants, and fixed with 4% PFA for 2 h at 4 °C.

4.6. Whole-mount immunohistofluorescence analysis and confocal imaging

The whole-mount immunohistofluorescence analysis was performed as previously described (Galindo-Romero et al., 2013). Briefly, the post-fixed retinas were washed 3 times in PBS, permeated in PBS with 0.5% Triton X100 by freezing them at −70 °C for 15 min, rinsed in new PBS with 0.5% Triton X100, and then incubated overnight with the primary antibodies at 4 °C. The primary antibodies used were rabbit anti-Iba1 (1:500, Wako Pure Chem. Indus.; Osaka, Japan), mouse anti-TNF-α antibody (1:50, Abcam; San Francisco, CA, USA), rabbit anti-GS antibody (1:1000, Abcam), and rabbit anti-GFAP antibody (1:1000, Abcam).

Next, after several washes, the retinas were incubated for 2 h at room temperature with the following secondary antibodies: either Alexa Fluor 488 dye-conjugated donkey anti-rabbit IgG (Invitrogen/Life Technologies; Carlsbad, CA, USA) or Alexa Fluor 555 dye-conjugated donkey anti-mouse IgG (Invitrogen/Life Technologies) at a 1:500 dilution in PBS with 0.5% Triton X100. Finally, the retinas were thoroughly washed in PBS, flat-mounted onto slides, and coverslipped in Vectashield mounting medium. To avoid fluorescence bleed-through caused by FG, the FG-labelled retinas were not coverslipped in Vectashield mounting medium. All images were captured with a confocal laser microscope (Carl Zeiss; Jena, Germany).

4.7. Quantification of RGCs and microglia

To count FG-labelled cells in the GCL, each retinal quadrant was divided into 3 areas by central, middle, and peripheral retina (one-sixth, three-sixths, and five-sixths of the retinal radius, respectively) as previously described (Lee et al., 2012). FG-labelled cells in 3 areas (0.18 mm^2 each) of each retinal quadrant were counted using the confocal laser microscope. The mean density of FG-labelled cells was calculated from the number of FG-labelled cells counted in the 12 areas of every retina. Iba1-, TNF-α-, GFAP- and GS-positive cells were also detected in the GCL within the same parameters as FG-labelled cells. Because the fragments of dying RGCs are phagocytosed by microglia which then become labelled with FG, FG-labelled microglia can also be identified and counted based on their morphology in the GCL. FG-labelled microglia can be easily differentiated from FG-labelled RGCs according to their size and shape (Baptiste et al., 2005; Slusar et al., 2013). RGCs have large circular or oval cell bodies (> 10 μm in diameter), whereas microglia are small, irregular rod-shaped or ameboid cells. RGCs and FG-labelled microglia in each image were manually counted along with Iba1-positive microglia.

4.8. Western blot analysis

On day 7 and 14 after ONT, the eyes were enucleated from the rats immediately after sacrifice, and retinal whole-mounts were collected, homogenized, and centrifuged at 12,000*g* for 15 min at 4 °C. The supernatants were collected, and their concentrations were determined by the BCA protein assay kit (Beyotime; Beijing, China). An equal amount of protein (50 μg) from each sample was resuspended in loading buffer, denatured at 95 °C for 5 min, separated by 12% sodium dodecyl sulfate-polyacrylamide gel electrophoresis (SDS-PAGE), and then transferred to polyvinylidene difluoride (PVDF) membranes (Millipore; Billerica, MA, USA). Next, the membranes were blocked and incubated with a primary antibody against TNF-α (1:1000, Abcam) at 4 °C overnight, with mouse anti-β-actin (1:5000, Millipore) used as an internal control. The bands were detected with a chemiluminescence reagent (ECL clarity, Bio-Rad; Hercules, CA, USA) and imaged by the ChemiDoc MP System (Bio-Rad). The bands' intensities were quantitatively analyzed using Image Lab Software (Bio-Rad).

4.9. Statistical analysis

Data were presented as the mean ± standard deviation (SD). Data and statistical analysis were performed using SPSS Statistical Software, version 17.0 (SPSS, Inc.; Chicago, IL, USA). Unpaired Student's *t*-test was used to determine significance between 2 groups, while 3 or more groups were analyzed by one-way analysis of variance (ANOVA) followed by a Tukey *post-hoc* test or a Dunnett's *post-hoc* test. Differences were considered significant when $p < 0.05$.

Conflict of interests

The authors declare that there is no conflict of interests regarding the publication of this article.

Authors' contributions

Participated in research design: HM Yin, HF Yin, and XY Fang. Conducted experiments: HM Yin, HF Yin, W Zhang, Q Miao, ZW Qin, SC Guo, JF Yin. Performed data analysis: HF Yin, QL Fu, J Ma. Wrote or contributed to the writing of the manuscript: HF Yin, F Wu and YB Yang. All authors have read and approved the final manuscript.

Acknowledgments

This paper was supported by the grant from the National Natural Science Foundation of China (81571819, 81300641 and 81300757); and by the grant from the Natural Science Foundation of Zhejiang Province (LY14H120004); and by the Program of Zhejiang Medical Technology (2015KYA109).

References

Ahmad, S., Elsherbiny, N.M., Bhatia, K., Elsherbini, A.M., Fulzele, S., Liou, G.I., 2014. Inhibition of adenosine kinase attenuates inflammation and neurotoxicity in traumatic optic neuropathy. J. Neuroimmunol. 277, 96–104.

Baptiste, D.C., Powell, K.J., Jollimore, C.A., Hamilton, C., LeVatte, T.L., Archibald, M.L., Chauhan, B.C., Robertson, G.S., Kelly, M.E., 2005. Effects of minocycline and tetracycline on retinal ganglion cell survival after axotomy. Neuroscience 134, 575–582.

Cen, L.P., Han, M., Zhou, L., Tan, L., Liang, J.J., Pang, C.P., Zhang, M., 2015. Bilateral retinal microglial response to unilateral optic nerve transection in rats. Neuroscience 311, 56–66.

Ciavatta, V.T., Kim, M., Wong, P., Nickerson, J.M., Shuler Jr., R.K., McLean, G.Y., Pardue, M.T., 2009. Retinal expression of Fgf2 in RCS rats with subretinal microphotodiode array. Investig. Ophthalmol. Vis. Sci. 50, 4523–4530.

Cuenca, N., Fernandez-Sanchez, L., Campello, L., Maneu, V., De la Villa, P., Lax, P., Pinilla, I., 2014. Cellular responses following retinal injuries and therapeutic approaches for neurodegenerative diseases. Prog. Retin. Eye Res. 43, 17–75.

Cueva Vargas, J.L., Osswald, I.K., Unsain, N., Aurousseau, M.R., Barker, P.A., Bowie, D., Di Polo, A., 2015. Soluble tumor necrosis factor alpha promotes retinal ganglion cell death in glaucoma via calcium-permeable AMPA receptor activation. J. Neurosci. 35, 12088–12102.

de Kozak, Y., Cotinet, A., Goureau, O., Hicks, D., Thillaye-Goldenberg, B., 1997. Tumor necrosis factor and nitric oxide production by resident retinal glial cells from rats presenting hereditary retinal degeneration. Ocul. Immunol. Inflamm. 5, 85–94.

Eder, C., 2005. Regulation of microglial behavior by ion channel activity. J. Neurosci. Res. 81, 314–321.

Eder, C., 2010. Ion channels in monocytes and microglia/brain macrophages: promising therapeutic targets for neurological diseases. J. Neuroimmunol. 224, 51–55.

Fujikado, T., Morimoto, T., Matsushita, K., Shimojo, H., Okawa, Y., Tano, Y., 2006. Effect of transcorneal electrical stimulation in patients with nonarteritic ischemic optic neuropathy or traumatic optic neuropathy. Jpn. J. Ophthalmol. 50, 266–273.

Galindo-Romero, C., Valiente-Soriano, F.J., Jimenez-Lopez, M., Garcia-Ayuso, D., Villegas-Perez, M.P., Vidal-Sanz, M., Agudo-Barriuso, M., 2013. Effect of brain-derived neurotrophic factor on mouse axotomized retinal ganglion cells and phagocytic microglia. Investig. Ophthalmol. Vis. Sci. 54, 974–985.

Gupta, N., Brown, K.E., Milam, A.H., 2003. Activated microglia in human retinitis pigmentosa, late-onset retinal degeneration, and age-related macular degeneration. Exp. Eye Res. 76, 463–471.

Henrich-Noack, P., Lazik, S., Sergeeva, E., Wagner, S., Voigt, N., Prilloff, S., Fedorov, A., Sabel, B.A., 2013. Transcorneal alternating current stimulation after severe axon damage in rats results in "long-term silent survivor" neurons. Brain Res. Bull. 95, 7–14.

Inomata, K., Shinoda, K., Ohde, H., Tsunoda, K., Hanazono, G., Kimura, I., Yuzawa, M., Tsubota, K., Miyake, Y., 2007. Transcorneal electrical stimulation of retina to treat longstanding retinal artery occlusion. Graefes Arch. Clin. Exp. Ophthalmol. 245, 1773–1780.

Isenmann, S., Kretz, A., Cellerino, A., 2003. Molecular determinants of retinal ganglion cell development, survival, and regeneration. Prog. Retin. Eye Res. 22, 483–543.

Karlstetter, M., Ebert, S., Langmann, T., 2010. Microglia in the healthy and degenerating retina: insights from novel mouse models. Immunobiology 215, 685–691.

Karlstetter, M., Scholz, R., Rutar, M., Wong, W.T., Provis, J.M., Langmann, T., 2015. Retinal microglia: just bystander or target for therapy? Prog. Retin. Eye Res. 45, 30–57.

Kitaoka, Y., Hayashi, Y., Kumai, T., Takeda, H., Munemasa, Y., Fujino, H., Ueno, S., Sadun, A.A., Lam, T.T., 2009. Axonal and cell body protection by nicotinamide adenine dinucleotide in tumor necrosis factor-induced optic neuropathy. J. Neuropathol. Exp. Neurol. 68, 915–927.

Kyung, H., Kwong, J.M., Bekerman, V., Gu, L., Yadegari, D., Caprioli, J., Piri, N., 2015. Celastrol supports survival of retinal ganglion cells injured by optic nerve crush. Brain Res. 1609, 21–30.

Lebrun-Julien, F., Duplan, L., Pernet, V., Osswald, I., Sapieha, P., Bourgeois, P., Dickson, K., Bowie, D., Barker, P.A., Di Polo, A., 2009. Excitotoxic death of retinal neurons in vivo occurs via a non-cell-autonomous mechanism. J. Neurosci. 29, 5536–5545.

Lee, D., Kim, K.Y., Noh, Y.H., Chai, S., Lindsey, J.D., Ellisman, M.H., Weinreb, R.N., Ju, W.K., 2012. Brimonidine blocks glutamate excitotoxicity-induced oxidative stress and preserves mitochondrial transcription factor a in ischemic retinal injury. PLoS One 7, e47098.

Lieberman, A.P., Pitha, P.M., Shin, H.S., Shin, M.L., 1989. Production of tumor necrosis factor and other cytokines by astrocytes stimulated with lipopolysaccharide or a neurotropic virus. Proc. Natl. Acad. Sci. USA 86, 6348–6352.

Liu, S., Li, Z.W., Weinreb, R.N., Xu, G., Lindsey, J.D., Ye, C., Yung, W.H., Pang, C.P., Lam, D.S., Leung, C.K., 2012. Tracking retinal microgliosis in models of retinal ganglion cell damage. Investig. Ophthalmol. Vis. Sci. 53, 6254–6262.

Miki, A., Kanamori, A., Negi, A., Naka, M., Nakamura, M., 2013. Loss of aquaporin 9 expression adversely affects the survival of retinal ganglion cells. Am. J. Pathol. 182, 1727–1739.

Miyake, K., Yoshida, M., Inoue, Y., Hata, Y., 2007. Neuroprotective effect of transcorneal electrical stimulation on the acute phase of optic nerve injury. Investig. Ophthalmol. Vis. Sci. 48, 2356–2361.

Morimoto, T., Miyoshi, T., Matsuda, S., Tano, Y., Fujikado, T., Fukuda, Y., 2005. Transcorneal electrical stimulation rescues axotomized retinal ganglion cells by activating endogenous retinal IGF-1 system. Investig. Ophthalmol. Vis. Sci. 46, 2147–2155.

Morimoto, T., Fujikado, T., Choi, J.S., Kanda, H., Miyoshi, T., Fukuda, Y., Tano, Y., 2007. Transcorneal electrical stimulation promotes the survival of photoreceptors and preserves retinal function in royal college of surgeons rats. Investig. Ophthalmol. Vis. Sci. 48, 4725–4732.

Morimoto, T., Miyoshi, T., Sawai, H., Fujikado, T., 2010. Optimal parameters of transcorneal electrical stimulation (TES) to be neuroprotective of axotomized RGCs in adult rats. Exp. Eye Res. 90, 285–291.

Ni, Y.Q., Gan, D.K., Xu, H.D., Xu, G.Z., Da, C.D., 2009. Neuroprotective effect of transcorneal electrical stimulation on light-induced photoreceptor degeneration. Exp. Neurol. 219, 439–452.

Okazaki, Y., Morimoto, T., Sawai, H., 2008. Parameters of optic nerve electrical stimulation affecting neuroprotection of axotomized retinal ganglion cells in adult rats. Neurosci. Res. 61, 129–135.

Pardue, M.T., Phillips, M.J., Yin, H., Sippy, B.D., Webb-Wood, S., Chow, A.Y., Ball, S.L., 2005. Neuroprotective effect of subretinal implants in the RCS rat. Investig. Ophthalmol. Vis. Sci. 46, 674–682.

Renz, H., Gong, J.H., Schmidt, A., Nain, M., Gemsa, D., 1988. Release of tumor necrosis factor-alpha from macrophages. Enhancement and suppression are dose-dependently regulated by prostaglandin E2 and cyclic nucleotides. J. Immunol. 141, 2388–2393.

Roh, M., Zhang, Y., Murakami, Y., Thanos, A., Lee, S.C., Vavvas, D.G., Benowitz, L.I., Miller, J.W., 2012. Etanercept, a widely used inhibitor of tumor necrosis factor-alpha (TNF-alpha), prevents retinal ganglion cell loss in a rat model of glaucoma. PLoS One 7, e40065.

Sato, T., Fujikado, T., Lee, T.S., Tano, Y., 2008. Direct effect of electrical stimulation on induction of brain-derived neurotrophic factor from cultured retinal Muller cells. Investig. Ophthalmol. Vis. Sci. 49, 4641–4646.

Schatz, A., Rock, T., Naycheva, L., Willmann, G., Wilhelm, B., Peters, T., Bartz-Schmidt, K.U., Zrenner, E., Messias, A., Gekeler, F., 2011. Transcorneal electrical stimulation for patients with retinitis pigmentosa: a prospective, randomized, sham-controlled exploratory study. Investig. Ophthalmol. Vis. Sci. 52, 4485–4496.

Schatz, A., Arango-Gonzalez, B., Fischer, D., Enderle, H., Bolz, S., Rock, T., Naycheva, L., Grimm, C., Messias, A., Zrenner, E., Bartz-Schmidt, K.U., Willmann, G., Gekeler, F., 2012. Transcorneal electrical stimulation shows neuroprotective effects in retinas of light-exposed rats. Investig. Ophthalmol. Vis. Sci. 53, 5552–5561.

Sharma, N., Marzo, S.J., Jones, K.J., Foecking, E.M., 2010. Electrical stimulation and testosterone differentially enhance expression of regeneration-associated genes. Exp. Neurol. 223, 183–191.

Sharma, P., Ping, L., 2014. Calcium ion influx in microglial cells: physiological and therapeutic significance. J. Neurosci. Res. 92, 409–423.

Siddiqui, A.M., Sabljic, T.F., Koeberle, P.D., Ball, A.K., 2014. Downregulation of BM88 after optic nerve injury. Investig. Ophthalmol. Vis. Sci. 55, 1919–1929.

Slusar, J.E., Cairns, E.A., Szczesniak, A.M., Bradshaw, H.B., Di Polo, A., Kelly, M.E., 2013. The fatty acid amide hydrolase inhibitor, URB597, promotes retinal ganglion cell neuroprotection in a rat model of optic nerve axotomy. Neuropharmacology 72, 116–125.

Tezel, G., Yang, X., Yang, J., Wax, M.B., 2004. Role of tumor necrosis factor receptor-1 in the death of retinal ganglion cells following optic nerve crush injury in mice. Brain Res. 996, 202–212.
Tonari, M., Kurimoto, T., Horie, T., Sugiyama, T., Ikeda, T., Oku, H., 2012. Blocking endothelin-B receptors rescues retinal ganglion cells from optic nerve injury through suppression of neuroinflammation. Investig. Ophthalmol. Vis. Sci. 53, 3490–3500.
Wang, J., Chen, S., Zhang, X., Huang, W., Jonas, J.B., 2015. Intravitreal triamcinolone acetonide, retinal microglia and retinal ganglion cell apoptosis in the optic nerve crush model. Acta Ophthalmol.
Wang, X., Mo, X., Li, D., Wang, Y., Fang, Y., Rong, X., Miao, H., Shou, T., 2011. Neuroprotective effect of transcorneal electrical stimulation on ischemic damage in the rat retina. Exp. Eye Res. 93, 753–760.
Wenjin, W., Wenchao, L., Hao, Z., Feng, L., Yan, W., Wodong, S., Xianqun, F., Wenlong, D., 2011. Electrical stimulation promotes BDNF expression in spinal cord neurons through Ca(2+)- and Erk-dependent signaling pathways. Cell. Mol. Neurobiol. 31, 459–467.
Yang, F., Wang, D., Wu, L., Li, Y., 2015. Protective effects of triptolide on retinal ganglion cells in a rat model of chronic glaucoma. Drug Des. Dev. Ther. 9, 6095–6107.
Yuan, T.F., Liang, Y.X., Peng, B., Lin, B., So, K.F., 2015. Local proliferation is the main source of rod microglia after optic nerve transection. Sci. Rep. 5, 10788.
Zeng, H.Y., Green, W.R., Tso, M.O., 2008. Microglial activation in human diabetic retinopathy. Arch. Ophthalmol. 126, 227–232.
Zheng, Z., Yuan, R., Song, M., Huo, Y., Liu, W., Cai, X., Zou, H., Chen, C., Ye, J., 2012. The toll-like receptor 4-mediated signaling pathway is activated following optic nerve injury in mice. Brain Res. 1489, 90–97.
Zhou, W.T., Ni, Y.Q., Jin, Z.B., Zhang, M., Wu, J.H., Zhu, Y., Xu, G.Z., Gan, D.K., 2012. Electrical stimulation ameliorates light-induced photoreceptor degeneration in vitro via suppressing the proinflammatory effect of microglia and enhancing the neurotrophic potential of Muller cells. Exp. Neurol. 238, 192–208.